INAF/OATs
LFI Project System Team

Planck LFI

TITLE: **Effect of bandpass on dipole calibration**

DOC. TYPE: Technical Note
PROJECT REF.: PL-LFI-OAT-TN-095 PAGE: 1 of 21
ISSUE/REV.: 1.0 DATE: 2015 May 25

Prepared by	M.Maris, T.Vassallo	2015 May 25
Agreed by	A.Zacchei	A.Zacchei
Approved by	A.Zacchei	

CHANGE RECORD

Issue	Date	Sheet	Description of change	Release
0.0	May 15th, 2015	All	First draft of document, provvisory number assigned	0.0
1.0	May 25th, 2015	All	definitve number assigned, first copy circulated	1.1

DISTRIBUTION LIST

Recipient	Company/Institute	E-mail address	Sent
Carlo Burigana	INAF/IASF-BO	burigana@iasfbo.inaf.it	May 25, 2015
Antony John Banday	MPA-Garching	banday@MPA-Garching.MPG.DE	May 25, 2015
Martin Reinecke	MPA-Garching	martin@MPA-Garching.MPG.DE	May 25, 2015
Tess Jaffe	CESR	tess.jaffe@cesr.fr	May 25, 2015
Andrea Zacchei	INAF-OATS	zacchei@oats.inaf.it	May 25, 2015
Fabio Finelli	INAF/IASF-BO	finelli@iasfbo.inaf.it	May 25, 2015
Alessandro Gruppuso	INAF/IASF-BO	gruppuso@iasfbo.inaf.it	May 25, 2015
Xi Chen	IPAC-Caltech	xchen@ipac.caltech.edu	May 25, 2015
Jose M. Diego	IFCA	jdiego@ifca.unican.es	May 25, 2015
Cecille Renault	IN	rcecile@in2p3.fr	May 25, 2015
Brendan Crill	JPL	Brendan.P.Crill@jpl.nasa.gov	May 25, 2015
Andrea Zonca	UCSB	zonca@deepspace.ucsb.edu	May 25, 2015

Contents

LIST OF ABBREVIATIONS

acronym	**Explanation**
LFI	Low Frequency Instrument
HFI	High Frequency Instrument
IDPs	Interplanetary Dust Particles
MOB	Mobile Object
SSB	Solar System Baricenter
SSO	Solar System Object
TBC	To Be Confirmed
TBD	To Be Defined
TOD	Time Ordered Data
TODs	Plural of TOD
TOI	Time Ordered Information
TODs	Plural of TOI
ZLE	Zodiacal Light Emission
DZLE	ZLE code from DIRBE WebSite
KZLE	Ken code for ZLE
HFIZLE	HFI residuals for ZLE
MZLE	Maris code for ZLE or My ZLE
ApJZLE	Paper ZLE model of Kelsall on ApJ
AXVZLE	Paper ZLE model of Kelsall on Archiv

1 Applicable and Reference Documents

Applicable Documents

[AD-1] Planck Collaboration,Aghanim, N., Armitage-Caplan, C. et al., 2014, *Planck 2013 results. V. LFI calibration* A&A, 571, A5 (also arxiv/1303.5066)

Reference Documents

[RD-1] Planck Collaboration,Aghanim, N., Armitage-Caplan, C. et al., 2014, *Planck 2013 results. V. LFI calibration* A&A, 571, A5 (also arxiv/1303.5066)

2 Scope of the document

The gain G in Planck is estimated on an pointing period basis by comparing the observed dipole amplitude with the expected dipole amplitude [AD-1]. So the ultimate accuracy in calibration is connected to the ability of the DPC to properly simulate the signal of the Cosmological Dipole. This in turn depends on the ability of DPC to properly calculate the proper `E4Pi` convolution parameters.

The `E4Pi` parameters are in turn computed from a GRASP model of beams and the QUCS model of bandpass. The bandpass model is affected by unknown level of uncertainties of which we want to estimate the impact on calibration and dipole residuals. Here we assumed a model of systematic uncertainty in banpasses and we propagate its effect on the maps through `E4Pi` convolution parameters.

2.1 Limits of Applicability

The results in this issue 2015 May 25, 1.0 of the document are subject to the following limitations:

1. This document represents just a case study to fix an order of magnitude of the effect of bandpass uncertainties.
2. The model variation of Bandpass is not based on any physical information about the radiometers, it is just an exemplification of the simplest possible variation.
3. The nominal bandpasses used are those distributed within DX11D release of LFI data inside the RIMO 2.4.
4. It is assumed that just the time dependent part of the dipole signal is relevant, the time independend part being removed by the destriping.

3 Analysis

The convolved dipole can be decomposed into a constant part and a time dependent part according to equation

$$\Delta T(\phi) = T_{\rm cmb}\frac{V_\odot}{c}S_h(\cos\beta_h\sin\hat{t} + \sin\beta_h + \cos\hat{t}\cos(\phi - \phi_{0,h}))); \quad (1)$$

where $T_{\rm cmb}$ the CMB temperature, $V_\odot$ the Solar System proper motion, S_h the smoothing factor introduced by convolution, ϕ is the phase describing the position of the beam on the scan circle, $\phi_{0,h}$ the phase in the reference position, $\hat{t}$ the angle between the spin axis and the dipole axis; β_h is the radius of the scan circle about the the spin axis.

The smoothing parameter S_h and the geometrical parameters $\phi_{0,h}$ and β_h describes the convolution process, different models of beam and bandpass will result in different values of those parameters. The uncertainties in the beam model and the bandpass will reflect in those values and consequently in gain uncertainties and residuals of dipole in the timelines.

It is assumed that just the time dependent part of the dipole signal is relevant, the time independend part being removed by the destriping.

3.1 Modeling the band pass uncertainties

To model the bandpass uncertainty we scaled the bandpass of each radiometer by scaling factor Y which changes linearly with the frequency according to

$$x(\nu) = \frac{\nu - \nu_0}{\nu_1 - \nu_0}; \quad (2)$$

$$Y_m(x) = \frac{1 + mx}{1 + m/2}; \quad (3)$$

$$(4)$$

where ν_0 and ν_1 are the minimal and maximal frequencies in the bandpass table.

It is important to stress that given $0 \leq x \leq 1$ and we must have $Y_m \geq 0$ for any x, then $-1 \leq m$, this makes the effects of $m = -1$ and $m = +1$ to be asymmetrical.

The scaled bandpass $\tau_m(\nu)$ is

$$\tau_m(\nu) = N_m Y_m(x(\nu))\tau(\nu); \quad (5)$$

with $\tau(\nu)$ the original bandpass, N_m a normalization constant to asses the integral of the modified bandpass to be 1.

The nominal case for the umodified bandpass corresponds to $m = 0$ and we will name it the *Fiducial* case, the $m \neq 0$ is named the *Test* case.

The modified bandpass was then used to generate a set of test `E4Pi` convolution parameters. Dipole signals are generated all over the mission with test parameters and Fiducial parameters.

Fig. 1 shows a tipical case of Test bandpass as a function of m, the ratio between Test bandpass and Fiducial bandpass is presented in Fig. 2.

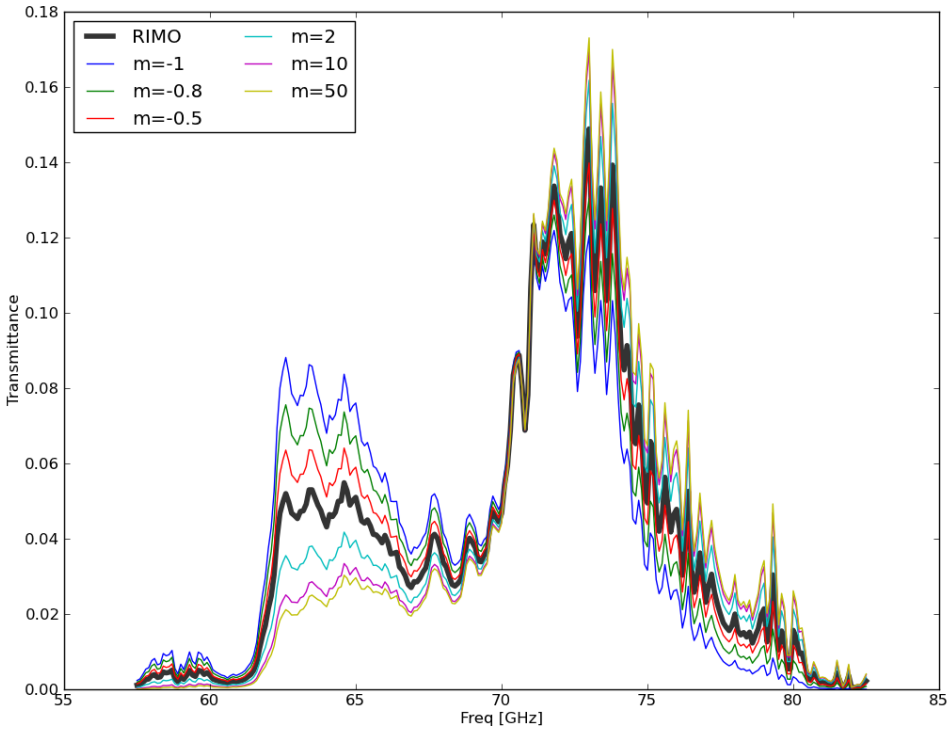

Figure 1: Test bandpass, here the RIMO is the Fiducial bandpass. It is evident the asymmetrical effect of positive and negative m.

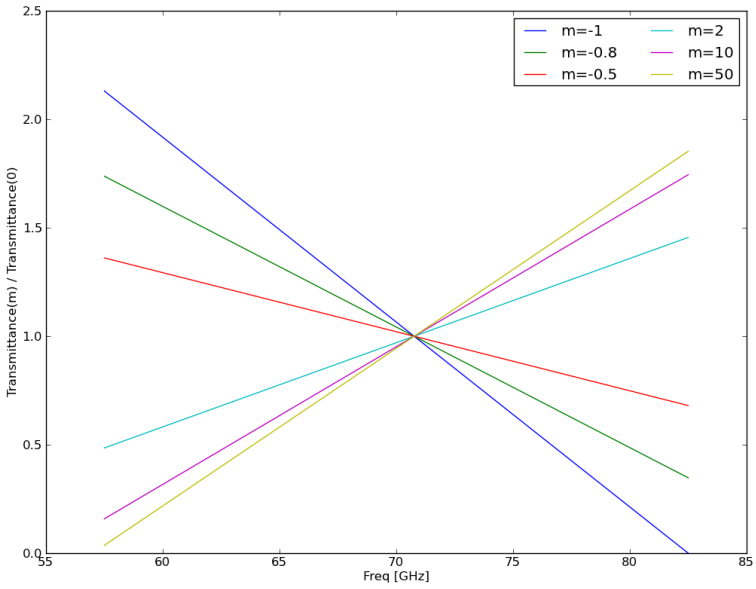

Figure 2: Test bandpass/Fiducial bandpass

4 Comparison procedure

4.1 Timelines

The comparison follows a quite simple logic, during calibration a Fiducial dipole have been used to calibrate a real dipole. In the ideal case, the only difference would be the fact that the real dipole is in Volts, due to the effect of the acquisition electronics, but in practice the real dipole differs from the Fiducial dipole, creating gain errors.

To investigate the gain differences we simply fit for each pointing period the Test dipole, coming from Test `E4Pi` parameters against the Fiducial dipole, coming from Fiducial `E4Pi` parameters, determining the best scaling factor G which minimizes

$$\chi^2 = \sum_t (GD_{\mathrm{test},t} - D_{\mathrm{fiducial},t})^2; \tag{6}$$

in case of no differences between Fiducial and Test case $G = 1$. Gain perturbations are simply $\delta G = (G - 1) \times 100$.

We also considered the residual dipole left in the toi of the pointing period in the case in which the real dipole is Test but it was removed as if it was Fiducial i.e.

$$r_{\mathrm{test},t} = GD_{\mathrm{test},t} - D_{\mathrm{fiducial},t}; \tag{7}$$

since this is a sinusoidal signal we will report just the amplitude of the residual sinusoid.

4.2 Maps

Fig. 11 presents three maps of dipole for one survey and one detector, with three different values of m. It is evident that the map is nothing else than a dipole.

The differences between dipoles convolved with different m for SS1 and SS2 and for horns 18, 24 and 27 are shown in Fig. 12, 13 and 14 respectively.

The difference formula is:

$$\mathcal{M}_{\mathrm{diff}} = \alpha \mathcal{M}_{\mathrm{test}} - \mathcal{M}_{\mathrm{fiducial}} \tag{8}$$

where $\mathcal{M}_{\mathrm{diff}}$, $\mathcal{M}_{\mathrm{test}}$ and $\mathcal{M}_{\mathrm{fiducial}}$ are the differences, test and fiducial maps α is the scaling factor already introduced for the differences of timelines.

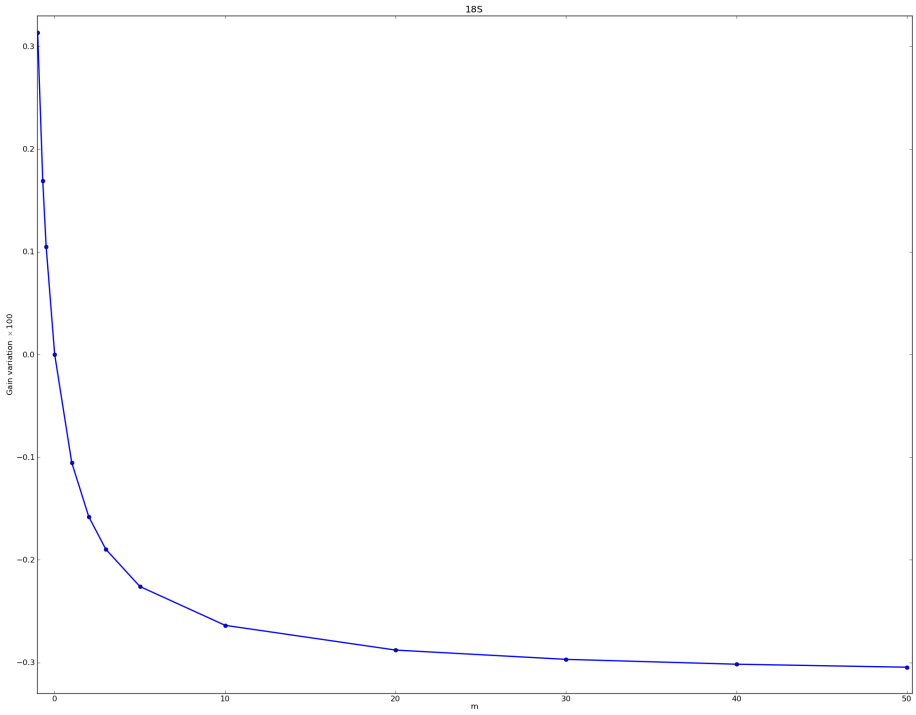

Figure 3: Gain change as a function of m for $-1 \leq m \leq +50$ for radiometer 18S.

5 Results

5.1 Timelines

Fig. 3 shows the gain change for 18S as a function of m. It is evident how increasing m the gain decreases with a trend which is the same for all the radiometers. Fig. 4 presents the range of changes for each radiometer for $-1 \leq m \leq 50$. The worst case allows for a gain change of about $\pm 0.3\%$. Also It is evident how 70 GHz frequency channes are the worst affected and the 44 GHz the least.

It has to be stressed as the gain change does not depend on time independent, the reason is that it is just a function of the difference of the `E4Pi` convolution parameters of Eq. (1) which is not time dependent.

Fig. 5 shows in the middle frame the how the amplitude of the residuals distributed over the od. In the worst case even 0.7 μK amplitude (i.e. 1.4 μK peak–to–peak) can be reached in some extreme cases when the dipole has its maximal amplitude. The residual amplitude follows 1–to–1 the dipole amplitude (see the top frame).

The last frame in the figure presents the ratio of the residual amplitude v.z. the dipole amplitude, since the G is time independent such ratio is time independent too, but its magnitude is

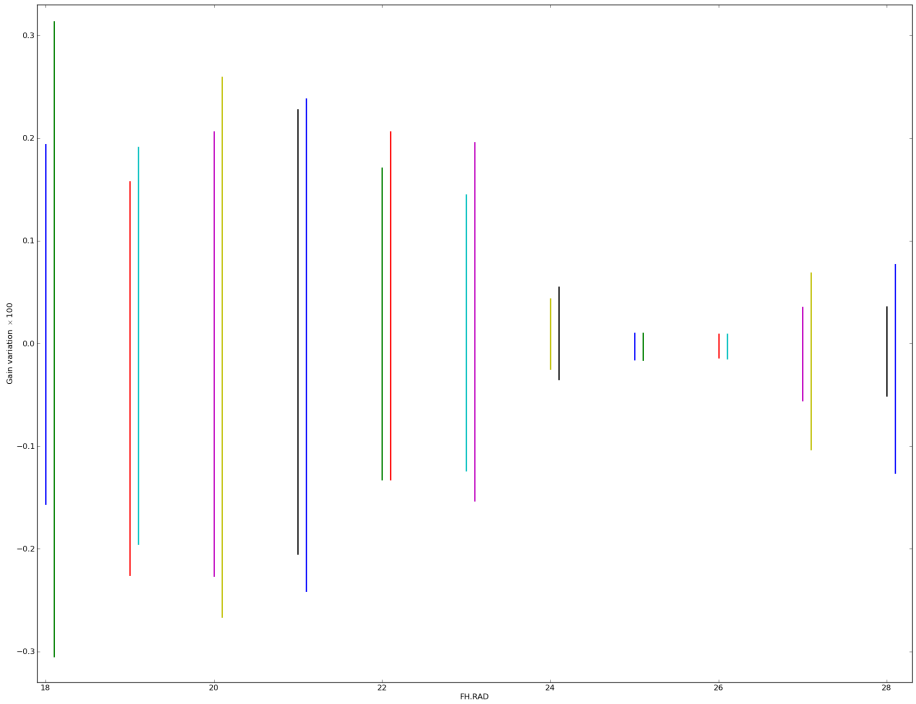

Figure 4: Range of variation of Gain for all of the radiometers, for $-1 \leq m \leq +50$.

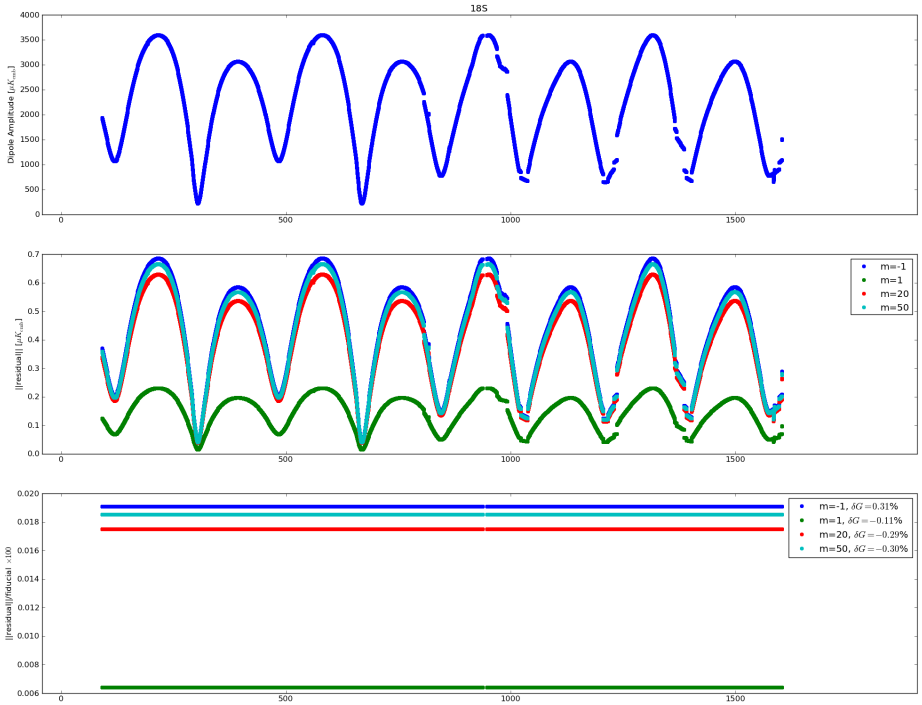

Figure 5: For radiometer 18S: top frame the fiducial dipole for each od, center frame the residual amplitude for various m, bottom frame the ratio of residual amplitude to the dipole amplitude.

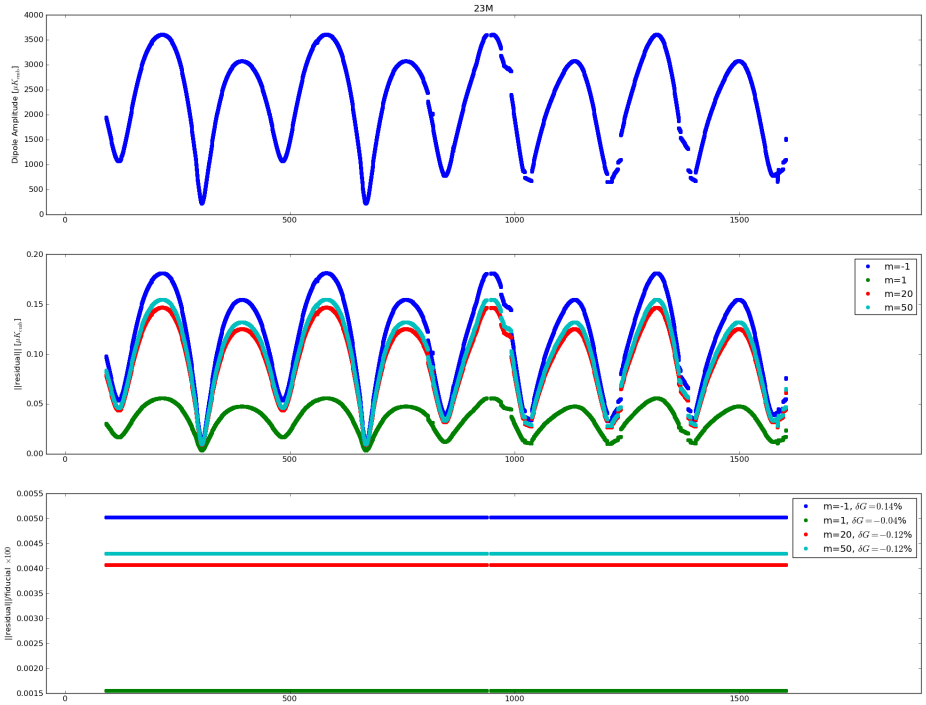

Figure 6: For radiometer 23S: top frame the fiducial dipole for each od, center frame the residual amplitude for various m, bottom frame the ratio of residual amplitude to the dipole amplitude.

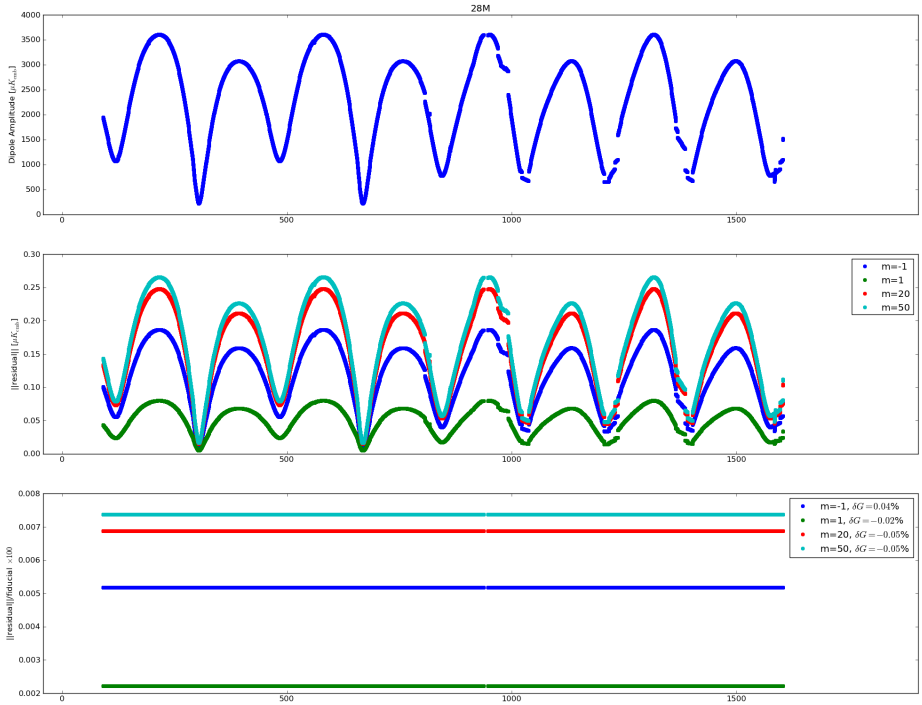

Figure 7: For radiometer 28M: top frame the fiducial dipole for each od, center frame the residual amplitude for various m, bottom frame the ratio of residual amplitude to the dipole amplitude.

about 10 - 20 times smaller than δG the reason is that the residual is mainly due to the slight differences in phases between Test and Fiducial dipoles. Would the phases be the same, residual would be zero even in case of large δG.

From the practical point of view a map of residuals would be nothing else than a scaled map of dipole.

As a further exemplification see Fig. 6 and Fig. 7 for other cases.

Figures 8, 9 and 10 shows how the residuals distributed for $m = -1$, 5 and 50 respectivelly. Each line spans over the minimum and maximum value of residual over the mission, the circle is the average.

By using Eq. (1) it is easy to understand why the residual is so small. Fitting the Fiducial agains the test will result in a gain which is

$$G = \frac{S'_h}{S_h}\frac{\hat{t}'_h}{\hat{t}_h}\cos(\phi 0, h' - \phi 0, h); \tag{9}$$

where the $'$ denotes the Test case. The application of G to the time dependent part of the Fiducial timeline results in a Fiducial dipole scaled to fit the test dipole. It is evident that if $\phi 0, h' = \phi 0, h$ the two timelines will be identical and no residual will be left, apart from a baseline which will be subsequenly removed by the destriping code, such exact cancellation will be not possible if the two phases are not identical the residual is proportional to

$$r_{\mathrm{test},t} \propto \underline{S'_h}$$

$${}'_h\hat{t}_h \cos(\phi 0, h' - \phi 0, h;$$

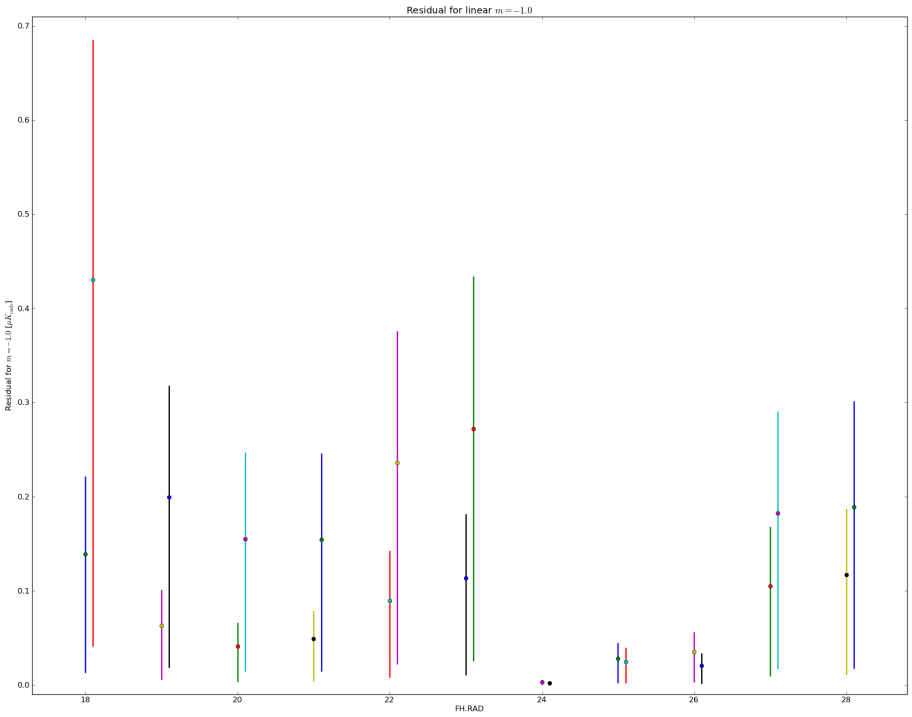

Figure 8: Min and Max residuals for each for m=-1, the circle is the mean over the whole mission.

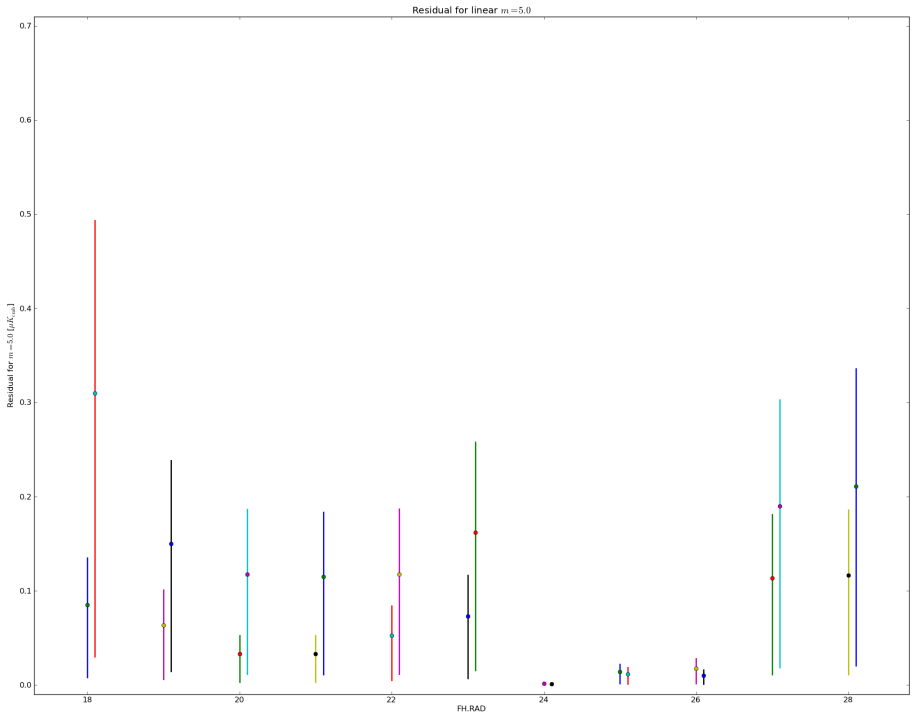

Figure 9: Min and Max residuals for each for m=5, the circle is the mean over the whole mission.

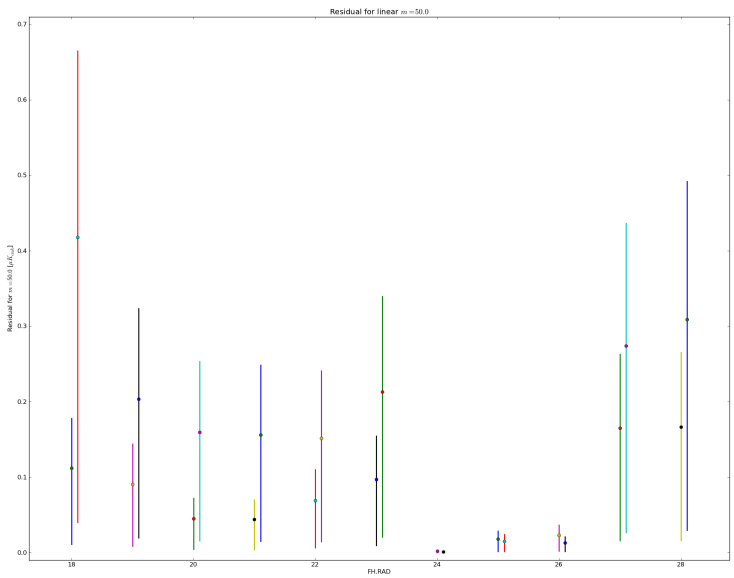

Figure 10: Min and Max residuals for each for m=50, the circle is the mean over the whole mission.

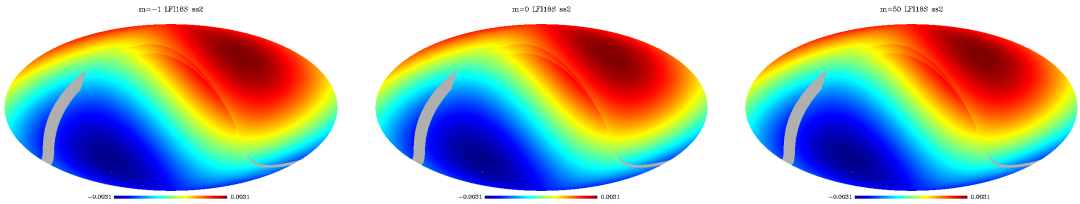

Figure 11: Maps of dipole for SS2 for $m = -1$, 0, +50 and detector 18S. The $m = 0$ case is the dipole with the nominal bandpass, maps are in Galactic coordinates.

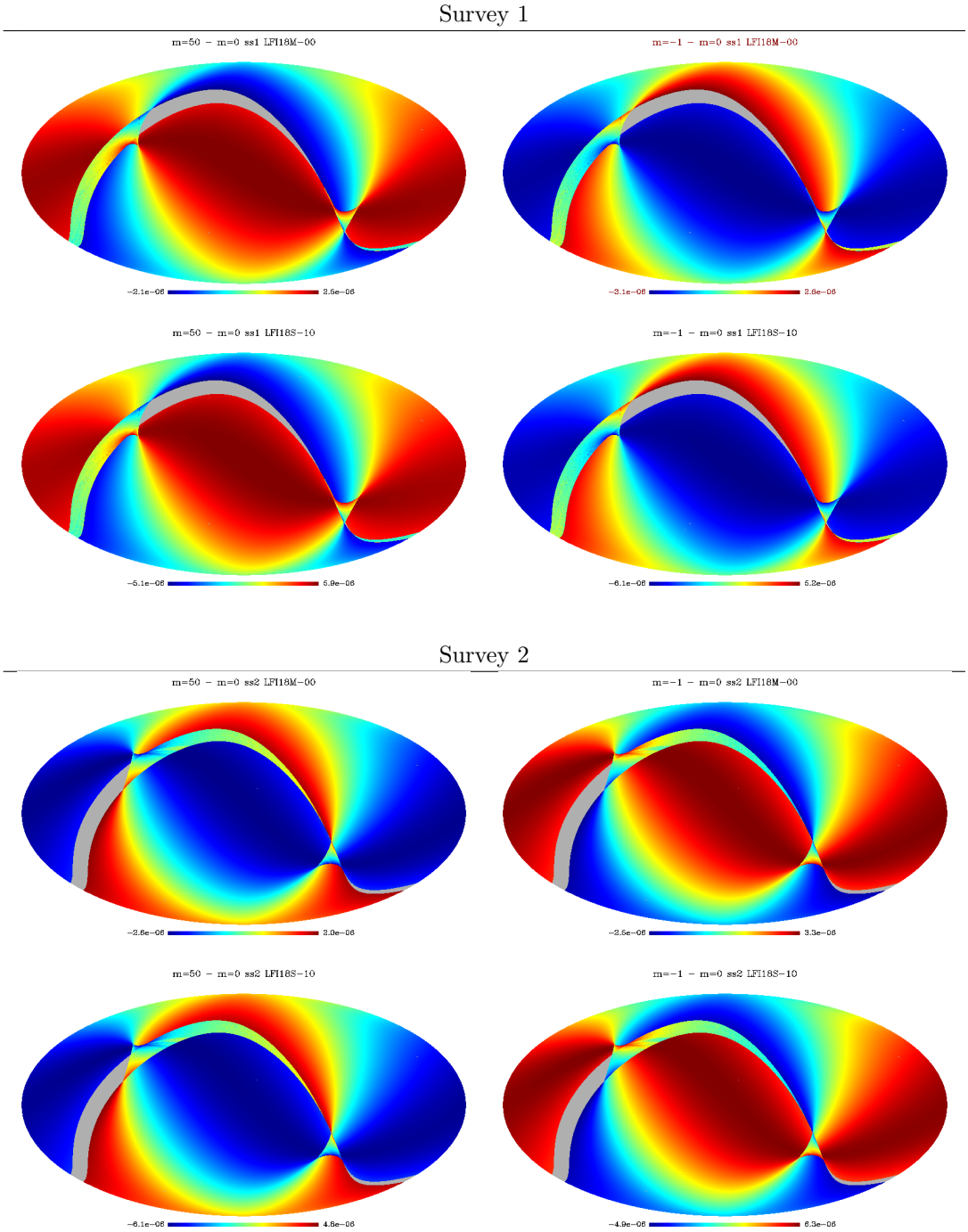

Figure 12: Differences for Survey 1 (top frame) and Survey 2 (bottom frame) between $m = 50$ and $m = 0$ (left) and $m = -1$ and $m = 0$ (right), for radiometers 18M (top row) and 18S (bottom row)

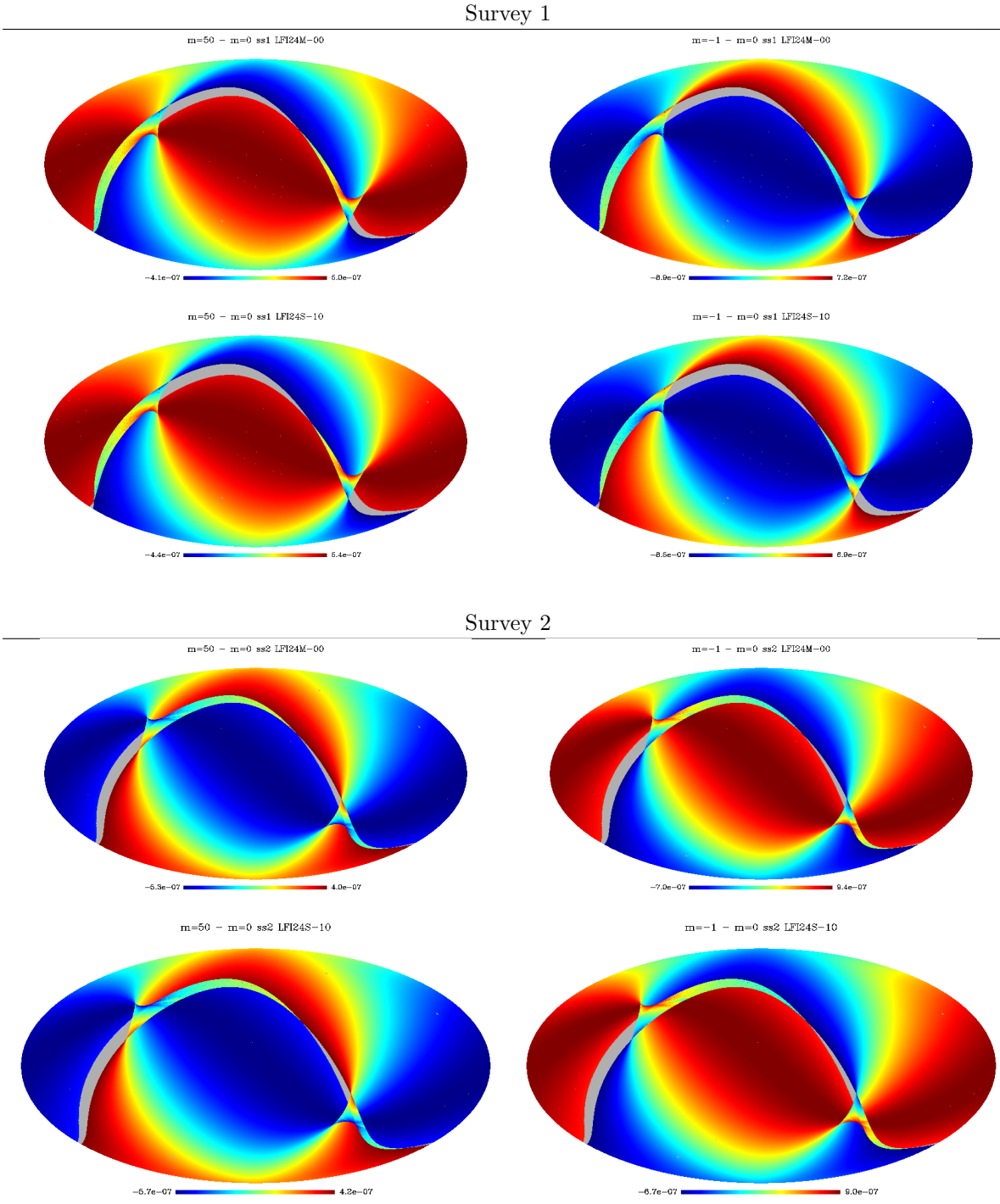

Figure 13: Differences for Survey 1 (top frame) and Survey 2 (bottom frame) between $m = 50$ and $m = 0$ (left) and $m = -1$ and $m = 0$ (right), for radiometers 24M (top row) and 24S (bottom row)

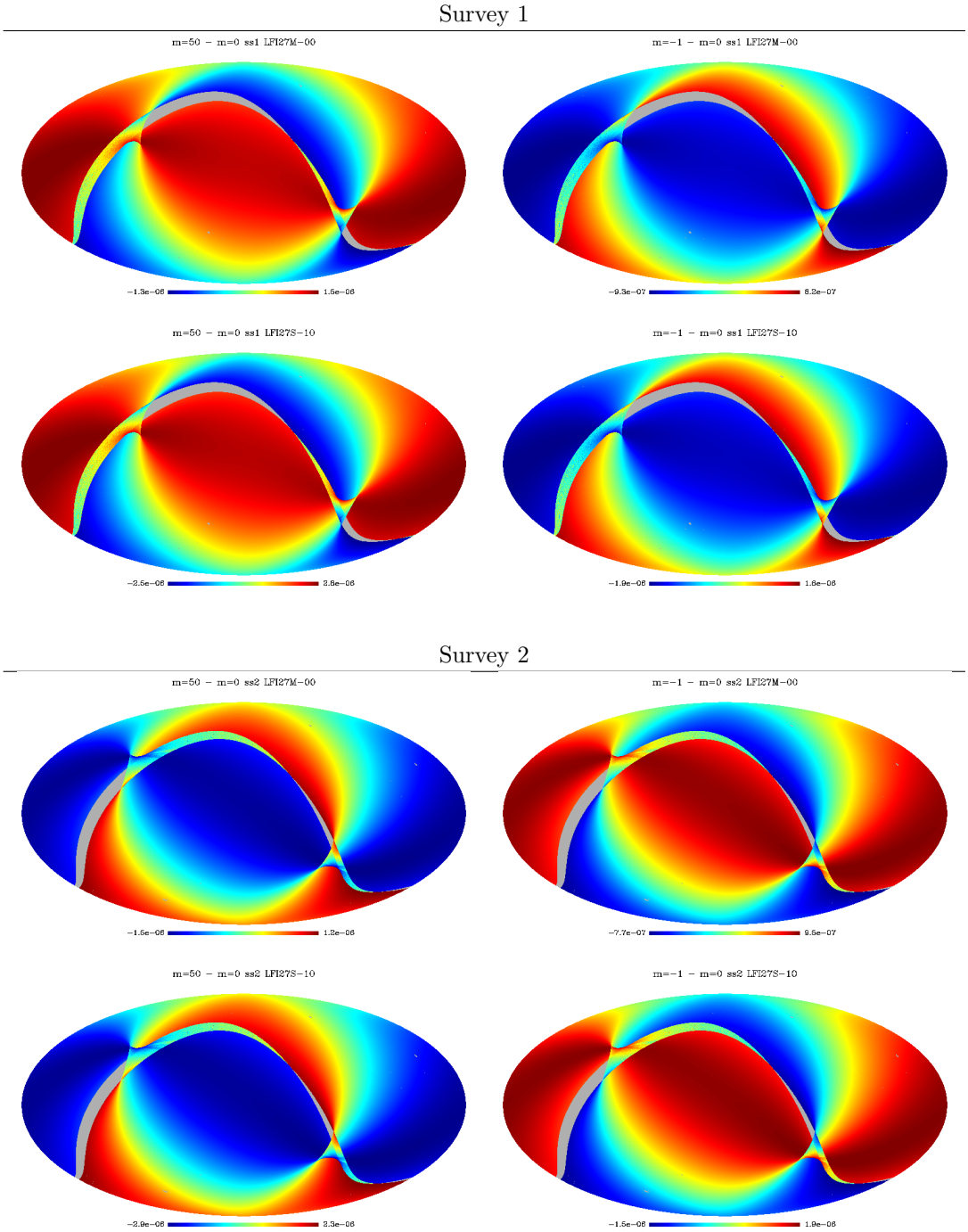

Figure 14: Differences for Survey 1 (top frame) and Survey 2 (bottom frame) between $m = 50$ and $m = 0$ (left) and $m = -1$ and $m = 0$ (right), for radiometers 27M (top row) and 27S (bottom row)

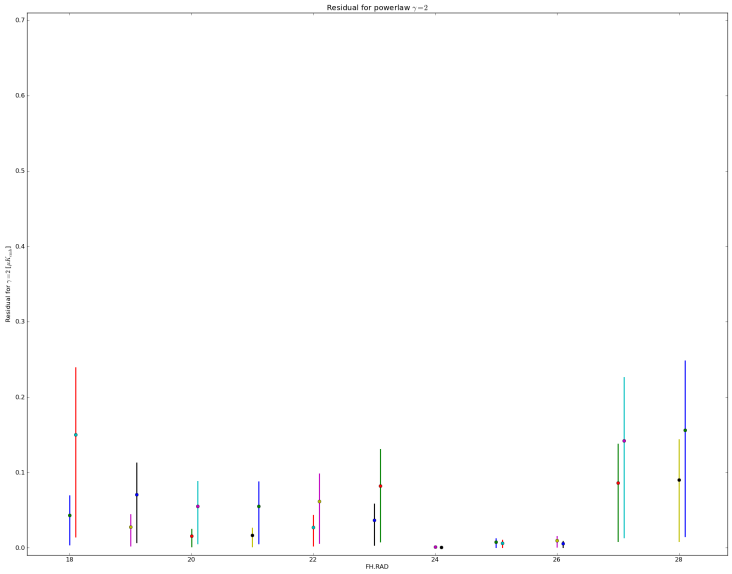

Figure 15: Min and Max residuals for a not flat spectrum of dipole.

6 Not flat spectrum of dipole

It is interesting also to compare this case with the systematic error we are introducing by assuming the dipole to be described by a flat spectrum. Indeed the dipole as seen from LFI is not flat, since it has a black body spectrum, this means that the high frequency side of the bandpass is overweighted with respect to the flat case. The residual left by this simplification can be seen in Fig. 15, as shown by the figure the effect is smaller than the most estreme cases of band distortion, but it is in line with the effect of more gentle band distortions.

7 Discussion

It is evident how the uncertainty in the bandpass could left residuals in the maps due to not proper dipole removal, of up to 0.7 μK.

However this is a worst case which should have to be constrained by some knowledge on the bandpass.

It is likely that the most important constrain can be obtained by introducing a solid constrain on the resulting central frequencies.

We also compared the effect of a bandpass distortion with the systematic error introduced by having considered the dipole has a source with a flat spectrum, the two systematics being comparable in their size.